HHS Public Access

Author manuscript

Neuromuscul Disord. Author manuscript; available in PMC 2020 October 09.

Published in final edited form as:

Neuromuscul Disord. 2010 June ; 20(6): 397–402. doi:10.1016/j.nmd.2010.04.004.

Neutral lipid storage disease with subclinical myopathy due to a retrotransposal insertion in the *PNPLA2* gene

Hasan O. Akman[a], **Guido Davidzon**[a], **Kurenai Tanji**[a,b], **Emma J. MacDermott**[c], **Louann Larsen**[c], **Mercy M. Davidson**[a], **Ronald G. Haller**[d], **Lidia S. Szczepaniak**[e], **Thomas J.A. Lehman**[c], **Michio Hirano**[a], **Salvatore DiMauro**[a,*]

[a]Department of Neurology, Columbia University Medical Center, New York, NY, USA

[b]Department of Pathology, Columbia University Medical Center, New York, NY, USA

[c]Department of Pediatric Rheumatology, Hospital for Special Surgery, New York, NY, USA

[d]Institute for Exercise and Environmental Medicine, Department of Neurology, VA Medical Center, and University of Texas Southwestern Medical Center, Dallas, TX, USA

[e]The Heart Institute at Cedars-Sinai Medical Center, Los Angeles, CA, USA

Abstract

An 18-year-old girl referred to a rheumatologist with malar flush and Gottran papules was found to have a markedly elevated serum CK. She was a good student and an avid ballet dancer. A muscle biopsy showed massive triglyceride storage, which was also found in peripheral blood granulocytes (Jordan anomaly) and cultured skin fibroblasts. Assessment using computerized dynamometry and cycle ergometry showed normal strength and muscle energetics, but proton spectroscopy revealed severe triglyceride accumulation in both skeletal and cardiac muscle. Sequencing of *PNPLA2*, the gene responsible for neutral lipid storage disease with myopathy (NLSDM), revealed a retrotransposal insertion of about 1.8 kb in exon 3 that abrogates transcription of *PNPLA2*. The sequences of *CGI-58*, the gene responsible for Chanarin–Dorfman syndrome (CDS), another multisystem triglyceride storage disease, and of two genes encoding lipid droplets-associated proteins, perilipin A and adipophilin, were normal. This case shows that NLSDM can be a transposon-associated disease and that massive lipid storage in muscle can present as asymptomatic hyperCKemia.

Keywords

Neutral lipid storage and myopathy; (NLSDM); Triglyceride lipase; HyperCKemia; *PNPLA2*; Retrotransposal insertion

*Corresponding author. Address: 4-424B College of Physicians & Surgeons, 630 West 168th Street, New York, NY 10032, USA. Tel.: +1 212 305 1662; fax: +1 212 305 3986., sd12@columbia.edu (S. DiMauro).

1. Introduction

Myopathies characterized by massive lipid storage are rare. The main causes of excessive accumulation of triglycerides (TG) in skeletal muscle are L-carnitine deficiency (both the systemic form and the much rarer myopathic form) [1], coenzyme Q_{10} (CoQ_{10}) deficiency [2], and two autosomal recessive multisystem TG storage diseases, Chanarin–Dorfman syndrome (CDS), also known as neutral lipid storage disease with ichthyosis (NLSDI), and neutral lipid storage disease with myopathy (NLSDM). NLSDM is due to mutations in the gene (*PNPLA2*) encoding a cytoplasmic adipose triglyceride lipase (ATGL) that catalyzes the first step in the hydrolysis of TG stored in lipid droplets [3]. CDS is due to mutations in the gene (*CGI-58* or *ABHD5*) encoding an activator of ATGL known as activator protein comparative gene identification 58 (*CGI-58*) [4]. Defects of long-chain fatty acid transport, such as carnitine palmitoyltransferase II (CPT II) deficiency, typically do not cause severe lipid storage, whereas multiple acyl-coenzyme A dehydrogenase deficiencies (MADD) due to defects in the genes encoding the electron transfer flavoprotein (ETF) or the ETF dehydrogenase (ETFDH) usually do [5,6].

We are following a completely asymptomatic18-year-old girl with persistently and markedly elevated serum CK. A muscle biopsy performed to unravel the cause of the hyperCKemia revealed massive TG storage, which was not confined to skeletal muscle, but also involved peripheral blood granulocytes and cultured skin fibroblasts. Proton spectroscopy showed excessive intracellular TG in the heart and, to a lesser extent, in liver. Although this patient is still completely asymptomatic, the pathological changes are so similar to those of NSLDM and CDS that we sequenced both genes and found a retrotransposon insertion in exon 3 of the *PNPLA2* gene, which presumably abolished mRNA synthesis and transcription. This case provides yet another example of a human transposon-mediated disease and raises two questions: (i) how can muscle maintain normal function in the face of massive lipid storage and persistent rhabdomyolysis? (ii) what is the long-term prognosis for this young woman?

2. Case report

Since age 10, this 18-year-old girl, the only daughter of consanguineous parents, showed malar flush, Gottren's papules in her hands and consistently elevated serum CK (1800–3000 IU; normal, <200), aldolase (27.5 IU; normal, 1–8), aspartate aminotransferase (AST) (94 IU, normal, <45), and alanine aminotransferase ALT (93 IU, normal, <45). The maternal grandmother had malar erythema, mildly increased serum CK without weakness, and had been diagnosed with SLE.

The malar rash and increased serum CK led to the diagnosis of dermatomyositis despite the lack of weakness, and she was treated with hydroxychloroquine, low-dose prednisone, infliximab, and cyclosporine, without any change in serum enzymes. A period of forced inactivity also failed to lower CK levels.

Other than the mild malar erythema, physical and neurological examinations were normal. She was an excellent student and a dedicated ballet dancer, practicing for several hours every week.

3. Methods

3.1. Histochemistry, biochemistry, and tissue culture

Histochemical studies of muscle using 8-mm-thick sections were carried out as described [7]. CoQ_{10} concentration in muscle was measured by reverse-phase high-performance liquid chromatography, as described [8]. Analysis of fatty acid oxidation was kindly performed in fibroblasts by Dr. Michael Bennett (Children's Hospital of Philadelphia). Skin fibroblasts were grown in glucose-rich Dulbecco's modified Eagle's medium (DMEM) supplemented with 10% fetal bovine serum, 1 ml fungizone, and 5 ml penicillin–streptomycin.

3.2. Cycle ergometry and Biodex system

Cycle exercise and oxidative capacity were determined employing an incremental cycle exercise protocol on a Lode Corival cycle ergometer with respiratory gas exchange measured using a Marquette 1100 medical gas analyzer. Maximal force generation in knee extension and flexion and in elbow flexion and extension were measured using a multi-joint computerized dynamometer. The patient's results were compared to those of three healthy control subjects of similar age.

3.3. Proton magnetic resonance spectroscopy

Intracellular lipid in the heart (ventricular septum), skeletal muscle (soleus), and the liver were determined using localized proton magnetic resonance spectroscopy conducted in a 1.5 Tesla Gyroscan INTERA whole body system (Philips Medical Systems, Best, The Netherlands). The technical details for measurement and evaluation of intracellular lipids have been described [9].

3.4. Molecular analysis

Total DNA was extracted from muscle by standard procedures (PUROGENE, Gentra System, Inc., Minneapolis, MN) according to the manufacturer's instructions. The genes for CGI-58, perilipin A, and adipophilin were sequenced by described techniques [4,10,11]. The entire coding sequence of *PNPLA2* was amplified by polymerase chain reaction using specific intron primers described by Fischer et al. [12]. To sequence the insertion, we used the following primers for the PCR amplification of exons 3 and 4: PNPLA2-Ex3F (5′-GACATGGGGCTATGAAGGAA-3′); PNPLA2-Ex3R (5′-AGG TGTCCAGGGCTAGGAAT-3′); PNPLA2-Ex4F (5′-CCCACTTCAACTCCAAGGAC-3′); PNPLA2-Ex4R (5′-TGCCACAGCTGTTTCTTGAG-3′). Thermal cycles were 95 °C for 5 min for initial denaturation; 35 cycles at 95° for 30 s each; 55 °C for annealing and 72 °C for extension.

3.5. Inverse PCR analysis

Genomic DNA (5 mg) was digested with *EaeI* and circularized with T4 DNA ligase (New England Biolabs, Beverly, MA). Circularized DNA fragments were amplified using the long template PCR kit (Roche Applied Science) with primers PNP51F (5′-CTGGTGCCAAGTTCATTGAG-3′) and PNP51R (5′-GCATACAGACCCTGGAGGAG-3′) synthesizing away from each other. The amplified

DNA fragments were isolated and sequenced using primer PNP52R (5′-GCTCACAGTTGGGACTTTGG-3′). To confirm the transposal insertion and for pedigree analysis, we performed PCR analysis using the following primers PNP5J1F (5′-TTGGGAAATACCAGGCAGAG-3′); PNP5J2R (5′-CCTCCCAGACAGGGTTGC-3′); and PNPLA2–32R (5′-AAGGCCAATGTCTGCAGCG-3′).

4. Results

4.1. Morphology and biochemistry

A left quadriceps muscle biopsy was snap frozen in isopentane–liquid nitrogen and cryosections were stained with a standard battery of histological and histochemical reactions, including oil Red O (ORO) and Nile Red. A profusion of intracellular lipid droplets staining intensely with Nile Red were present in both fiber types, more abundantly in type I fibers (Fig. 1A and B). Scattered fibers were mildly atrophic but there was no fiber type grouping. There were neither rimmed vacuoles nor any increase in acid phosphatase staining. The modified Gomori trichrome stain failed to reveal any ragged-red fibers. Skin fibroblasts, obtained by punch biopsy from the patient, her parents, and her maternal grandmother, were cultured to confluency in standard media. Nile Red staining showed marked cytoplasmic lipid accumulation in the patient's fibroblasts (Fig. 1C and D) and milder accumulation in fibroblasts from her parents and grandmother compared to control cells. A peripheral blood smear revealed extensive vacuolization of granulocytes (Jordan anomaly) (Fig. 2).

Total carnitine concentration in blood was normal, and the concentration of CoQ_{10} in muscle was actually increased (83.0 μg/g; normal, 32.1 ± 6.6). Fatty acid oxidation in fibroblasts showed about 50% reduction in the utilization of palmitate, which was not considered sufficient to cause such a severe TG storage.

4.2. Exercise physiology and proton magnetic resonance spectroscopy

Cycle exercise, oxidative capacity, and strength assessment were similar in the patient and in all three age-matched normal women.

By localized proton magnetic resonance spectroscopy, intracellular lipid levels were dramatically higher in skeletal muscle (approximately 20 times the mean value of the age- and gender-matched controls) and the myocardium (approximately 10 times the mean control values) and moderately higher in liver (approximately three times the control mean but still in the normal range) (Fig. 3).

4.3. Molecular genetics

The genes encoding CGI-58, perilipin, and adipophilin were normal. Sequencing of the *PNPLA2* gene showed that all exons and promoter regions were normal, but exon 3 yielded no PCR product. Fig. 4A shows the normal exon 4 amplicon from DNA samples of the patient, her mother, and her grandmother but the lack of amplification of exon 3 with the patient's DNA. RT-PCR failed to amplify the patient's PNPLA2 mRNA. Since exons 3 and 4 are very close, and neither reverse primer could amplify exon 3, we used the inverse PCR

technique to amplify the unknown sequence downstream of exon 3. This allowed us to use the known region upstream of exon 3, where we used primers PNPLA2–51F and PNPLA2–51R for PCR amplification (illustrated in Fig. 4B). Sequencing the amplified segment with PNPLA2–52R identified the insertion point and duplication of the 12 bp 5′-AAAGAGGCCCGG segment of exon 3 (Fig. 4C). Detection of the insertion point led us to design a new PCR to test the parents and the patient for this genetic change, by synthesizing a reverse primer, 523 bp downstream of the insertion point. In the presence of the mutation, the primers amplified a fragment 222 bp larger than the normal exon 3, and the two fragments were easily distinguished by standard agarose gel electrophoresis (Fig. 4D). PCR analysis of genomic DNA from the parents and the grandmother revealed that they are heterozygous (Fig. 4D) and allowed us to draw a pedigree (Fig. 4E).

4.3.1. Identification of the DNA fragment inserted in exon 3—The insertion in exon 3 (1.8 kb in length) has been amplified by PCR and sequenced (Fig. 5). Analysis of this sequence by BLAST search of Genbank sequences identified five characteristic elements of an SVA retrotransposon: (i) *Alu*-like sequences that start at the insertion point and continue for the next 517 bases; (ii) 868-bp long variable tandem repeats, which are highly (78%) GC-rich; (iii) interspersed 431-bp short nucleotide elements; (iv) poly dA 44 bp-long or 340 bp-long dA-rich regions; (v) these groups of four elements begin and end with 12-bp 5′-AAAGAGGCCCGG-3′, the duplicated fragments shown schematically in red in Fig. 5.

5. Discussion

The severe TG storage in this girl was an unexpected finding in a muscle biopsy performed to pursue the cause of a marked and persistent hyperCKemia that was not related to exercise. Aside from a mild malar flush, also present in her maternal grandmother, the patient was asymptomatic. In particular, she showed no weakness by manual testing using the computerized dynamometry or by cycle ergometry: in fact, she was a devoted ballet dancer. The mild accumulation of TG in cultured skin fibroblasts from her mother and grandmother suggested that they may be carriers of an autosomal recessive mutation in a gene involved in TG metabolism.

Carnitine deficiency causes lipid storage myopathy. In the more common systemic variant, due to genetic defects of the cell membrane organic cation transporter (*OCTN2*), there is also involvement of other tissues, with low serum carnitine, proximal weakness, cardiomyopathy, and hepatomegaly [1]. In the much less common myopathic variant, there is only a fluctuating proximal myopathy and the molecular defect remains unclear [13]. Both variants respond to L-carnitine supplementation. The lack of weakness and the normal serum carnitine concentration excluded the systemic form and made the myopathic form unlikely.

Apparently primary CoQ_{10} deficiency is another cause of lipid storage myopathy, which can be isolated [2,14] or associated with central nervous system dysfunction manifested by seizures, ataxia, or mental retardation [15–17]. However, the lipid storage is invariably accompanied by mitochondrial proliferation with ragged-red fibers (RRF). The lack of

weakness and RRF in the muscle biopsy of our patient was against the diagnosis of CoQ_{10} deficiency, which was excluded by direct measurement of CoQ_{10} in muscle.

The multisystem nature of the TG storage, first suggested by the vacuolar appearance of granulocytes in a peripheral blood smear (the so called Jordan anomaly) and confirmed by Nile Red staining of cultured skin fibroblasts, suggested the diagnosis of Chanarin–Dorfman syndrome (CDS). CDS, first described by Rozenszajn in 1966 [18], has been reported in about 30 patients and is characterized clinically by ichthyosis, an obligatory sign (hence the term neutral lipid storage disease with ichthyosis, or NLSDI, currently used for this disease), and, less consistently, hepatomegaly, chronic diarrhea with steatorrhea, myopathy with variably elevated serum CK, ataxia, neurosensory hearing loss, subcapsular cataracts, and ectropion [4,19,20]. Although our patient had none of the clinical signs of NLSDI, we sequenced the *CGI-58* gene and found no pathogenic mutations.

In adipocytes, CGI-58 localizes to the lipid droplets and is associated with perilipin A, a phosphoprotein coating the phospholipid surface membrane of lipid droplets and involved in cAMP-dependent lipolysis. Perilipin A is but one member of a family of lipid droplet-associated proteins, called PAT from their initials: perilipin, ADPR (adipocyte-differentiation-related protein, also called adipophilin) and TIP-47 [21]. Therefore, we also sequenced the genes encoding perilipin and adipophilin, but failed to identify pathogenic mutations.

A second form of NLSD is dominated clinically by progressive myopathy (NLSDM) and is due to mutations in the gene (*PNPLA2*) that encodes another neutral TG lipase, also bound to the lipid droplets and working hand-in-hand with the CGI-58 protein [3]. Both disorders result in massive lipid storage in all tissues but especially in skeletal muscle. In addition to lipid storage, patients with NLSDM often show myopathic features, notably rimmed vacuoles [6,22], which were absent in our patient. Despite the congenital nature of these disorders, muscle weakness in NLSDM typically starts in young adult life [22,23].

In our patient, we found that exon 3 of the *PNPLA2* gene was interrupted by a 1.8 kb DNA insertion, which was identified as a retrotransposon fragment. This retrotransposal sequence has a long dT- and dA-rich region that is likely to either slow down or block altogether the transcription mediated by RNApol II. A second impediment to transcription is the presence of very GC-rich variable tandem repeats (VTR), which are a hallmark of SVA transposons. Taken together, these features explain why we failed to amplify any cDNA from total RNA extracted from leukocytes or fibroblasts of our patient. SVA transposons are the least studied mobile elements and only a few have been associated with disease, including Fukuyama-type muscular dystrophy [24,25].

This case raises several interesting questions. First, it shows that massive lipid storage in muscle fibers does not interfere with contractile function and muscle energetics, as the patient's strength was unaffected. This observation casts some doubt on the mechanical role of storage material, be it fat or glycogen, in causing muscle weakness. Second, it poses the crucial clinical dilemma of prognosis. Two considerations make it very likely that this young woman will develop weakness later in her life: (i) a review of the six cases with *PLPLA2*

mutations reported in detail thus far shows that weakness usually starts in the 30s and never before age 20 [22,23,26]; and (ii) the severe lipid accumulation already evident in various organs, including the heart, while still clinically silent, is likely to cause symptoms in the long run. A third, and related question, is if and how we can intervene pharmacologically to protect her from the expected deleterious effects of her storage disease. We are planning *in vitro* studies using the TG storage in her cultured fibroblasts as biomarker to monitor the effects of dietary regimens and pharmacological agents.

Acknowledgements

This work was supported by grants from the Muscular Dystrophy Association (RGH and SDM) and the VA Merit Review (RGH). The authors are grateful to Phil Wyrick, M.A., and Marta Newby, R.N. for their expert assistance.

References

[1]. Tein I Carnitine transport: pathophysiology and metabolism of known molecular defects. J Inher Metab Dis 2003;26:147–69. [PubMed: 12889657]

[2]. Horvath R, Scneiderat P, Schoser BGH, et al. Coenzyme Q10 deficiency and isolated myopathy. Neurology 2006;66:253–5. [PubMed: 16434667]

[3]. Zimmermann R, Strauss JG, Haemmerle G, et al. Fat mobilization in adipose tissue is promoted by adipose triglyceride lipase. Science 2004;306:1383–6. [PubMed: 15550674]

[4]. Lefevre C, Jobard F, Caux F, et al. Mutations in *CGI-58*, the gene encoding a new protein of the esterase/lipase/thioesterase subfamily, in Chanarin–Dorfman syndrome. Am J Hum Genet 2001;69:1002–12. [PubMed: 11590543]

[5]. Gempel K, Topaloglu H, Talim B, et al. The myopathic form of coenzyme Q10 deficiency is caused by mutations in the electron-transferring-flavoprotein dehydrogenase (ETFDH) gene. Brain 2007;130:2037–44. [PubMed: 17412732]

[6]. Ohkuma A, Noguchi S, Sugie H, et al. Clinical and genetic analysis of lipid storage myopathies. Muscle Nerve 2009;39:333–42. [PubMed: 19208393]

[7]. Tanji K, Bonilla E. Optical imaging techniques (histochemical, immunohistochemical, and in situ hybridization staining methods) to visualize mitochondria. Methods Cell Biol 2001;65:311–32. [PubMed: 11381601]

[8]. Lamperti C, Naini AB, Lucchini V, et al. Muscle coenzyme Q10 in statin-related myopathy. Arch Neurol 2005;62:1709–12. [PubMed: 16286544]

[9]. Szczepaniak LS, Babcock EE, Schick F, et al. Measurement of intracellular triglyceride stores by H spectroscopy: validation in vivo. Am J Physiol 1999;276:E977–89. [PubMed: 10329993]

[10]. Wolins NE, Quaynor BK, Skinner JR, Schoenfish MJ, Tzekov A, Bickel PE. S3–12, adipophilin, and TIP-47 package lipid in adipocytes. J Biol Chem 2005;280:19146–55. [PubMed: 15731108]

[11]. Subramanian V, Rothenberg A, Gomez C, et al. Perilipin A mediates the reversible binding of CGI-58 to lipid droplets in 3T3-L1 adipocytes. J Biol Chem 2004;279:42062–71. [PubMed: 15292255]

[12]. Fischer J, Lefevre C, Morava E, et al. The gene encoding adipose triglyceride lipase (PNLPA2) is mutated in neutral lipid storage disease with myopathy. Nat Genet 2007;39:28–30. [PubMed: 17187067]

[13]. Tein I Lipid storage muscular disorders In: Jones HR, De Vivo DC, Darras BT, editors. Neuromuscular disorders of infancy, childhood, and adolescence, vol. 1 Boston: Butterworth–Heinemann; 2003 p. 833–60.

[14]. Lalani S, Vladutiu GD, Plunkett K, Lotze TE, Adesina AM, Scaglia F. Isolated mitochondrial myopathy associated with muscle coenzyme Q10 deficiency. Arch Neurol 2005;62:317–20. [PubMed: 15710863]

[15]. Ogasahara S, Engel AG, Frens D, Mack D. Muscle coenzyme Q deficiency in familial mitochondrial encephalomyopathy. Proc Natl Acad Sci USA 1989;86:2379–82. [PubMed: 2928337]

[16]. Sobreira C, Hirano M, Shanske S, et al. Mitochondrial encephalomyopathy with coenzyme Q10 deficiency. Neurology 1997;48:1238–43. [PubMed: 9153450]

[17]. Di Giovanni S, Mirabella M, Spinazzola A, et al. Coenzyme Q10 reverses pathological phenotype and reduces apoptosis in familial CoQ10 deficiency. Neurology 2001;57:515–8. [PubMed: 11502923]

[18]. Rosenszajn L, Klajman A, Yaffe D, Efrati P. Jordan's anomaly in white blood cells: report of a case. Blood 1966;28:258–65. [PubMed: 5330405]

[19]. Miranda AF, DiMauro S, Eastwood AB, et al. Lipid storage, ichthyosis, and steatorrhea. Muscle Nerve 1979;2:1–13. [PubMed: 545139]

[20]. Bruno C, Bertini E, Di Rocco M, et al. Clinical and genetic characterization of Chanarin–Dorfman syndrome. Biochem Biophys Res Commun 2008;369:1125–8. [PubMed: 18339307]

[21]. Londos C, Sztalryd C, Tansey JT, Kimmel AR. Role of PAT proteins in lipid metabolism. Biochemie 2005;87:45–9.

[22]. Ohkuma A, Nonaka I, Malicdan MC, et al. Distal lipid storage myopathy due to *PNPLA2* mutation. Neuromuscul Disord 2008;18:671–4. [PubMed: 18657972]

[23]. Campagna F, Nanni L, Quagliarini F, et al. Novel mutations in the adipose triglyceride kinase gene causing neutral lipid storage diseases with myopathy. Biochem Biophys Res Commun 2008;377:843–6. [PubMed: 18952067]

[24]. Kobayashi K, Nakahori Y, Miyake M, et al. An ancient retrotransposal insertion causes Fukuyama-type congenital muscular dystrophy. Nature 1998;394:388–92. [PubMed: 9690476]

[25]. Mills RE, Bennett EA, Iskow RC, Devine SE. Which transposable elements are active in the human genome? Trends Genet 2007;23:183–91. [PubMed: 17331616]

[26]. Akiyama M, Sakai K, Ogawa M, McMillan JR, Sawamura D, Shimizu H. Novel duplication mutation in the patatin domain of adipose triglyceride lipase (PNPLA2) in neutral lipid storage disease with severe myopathy. Muscle Nerve 2007;36:856–9. [PubMed: 17657808]

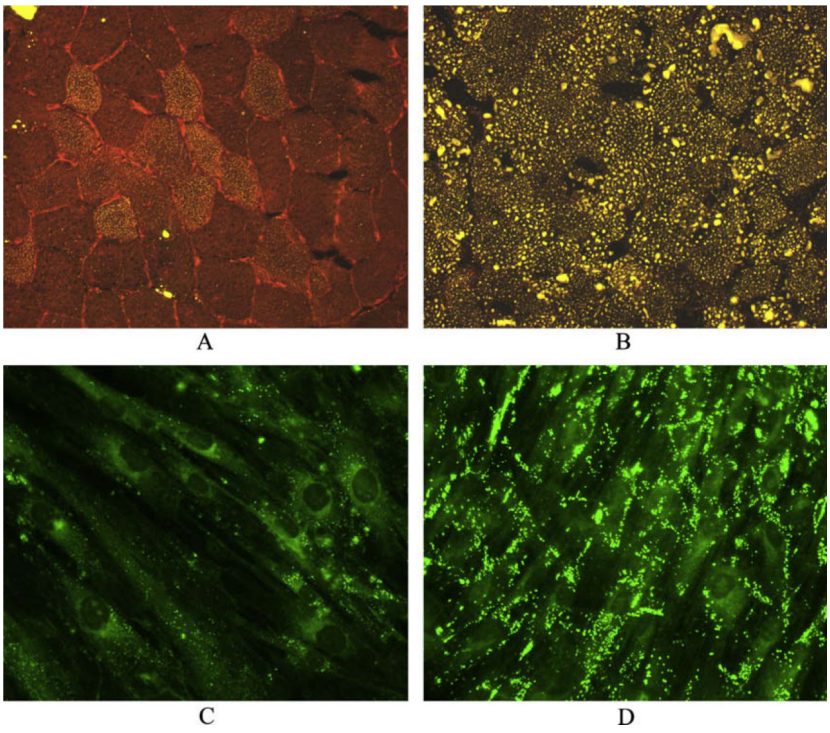

Fig. 1.

Nile Red stain of muscle cryosections (A and B) and of confluent cultured skin fibroblasts (C and D) showing the marked increase in lipid droplets in the patient's muscle (B) and fibroblasts (D) than in control tissues (A and C).

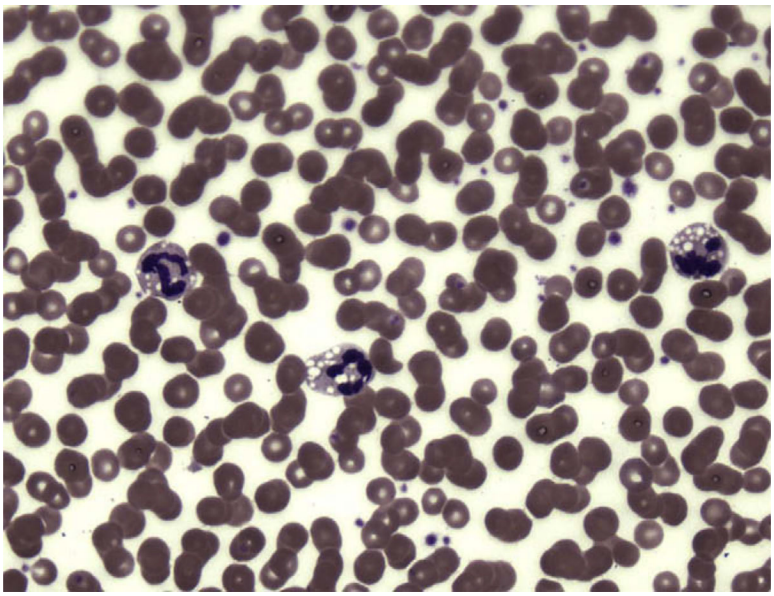

Fig. 2.
Vacuolization of granulocytes (Jordan anomaly) in a peripheral blood smear from the patient.

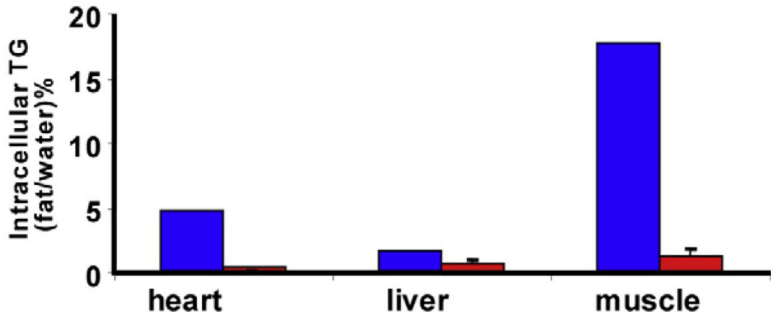

Fig. 3.

Intracellular triglyceride measured by proton spectroscopy in myocardium, skeletal muscle and liver from the patient and three controls (the bars indicate SD). The values in the patient were far above average values for morbidly obese adults.

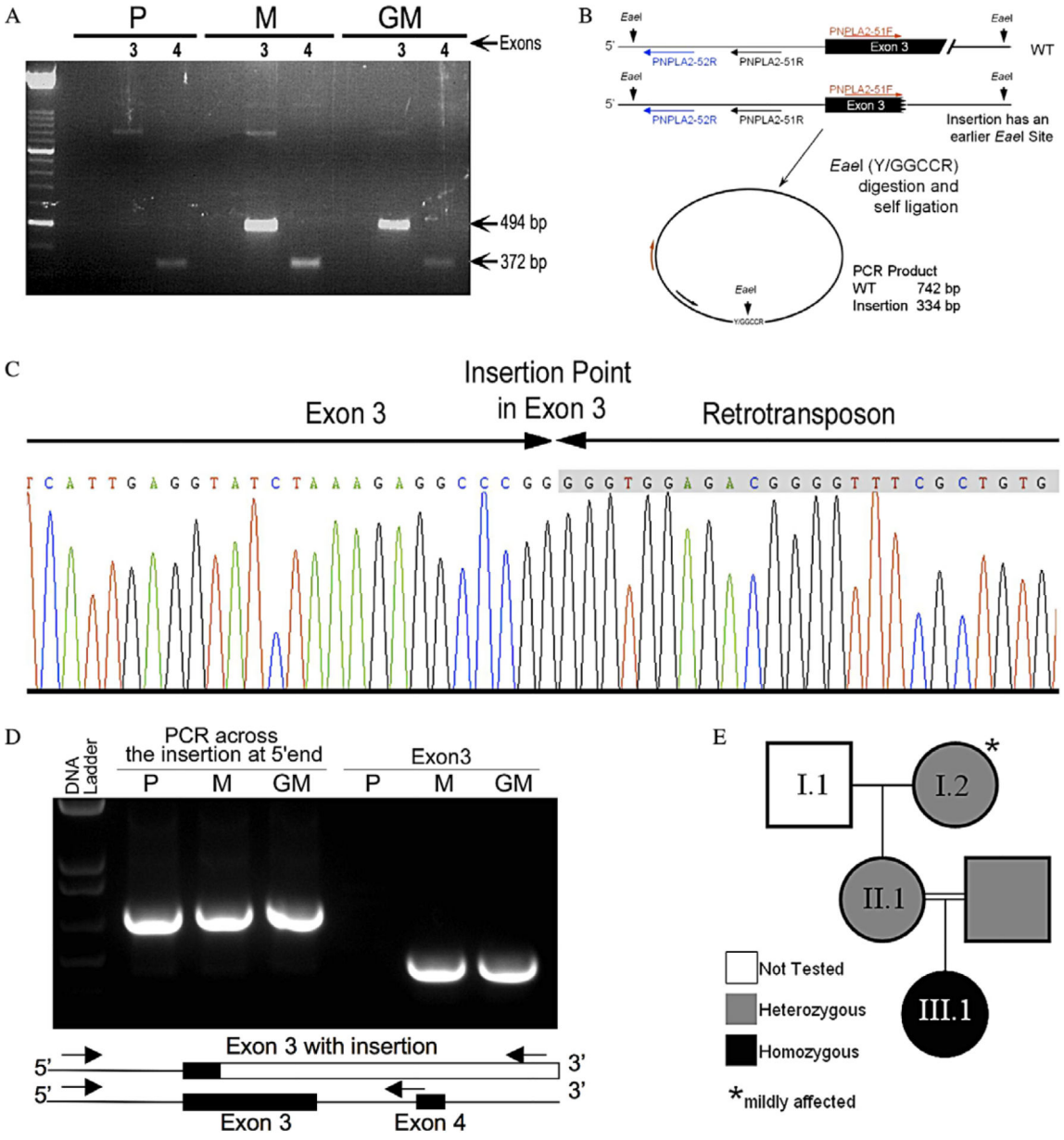

Fig. 4.

Molecular analysis of the PNPLA2 gene. (A) PCR amplification of exons 3 and 4 of the *PNPLA2* gene from the genomic DNA of the patient (P), her mother (M), and grandmother (GM). (B) Diagram of the inverse PCR reaction strategy. (C) Electropherogram of inverse PCR products shows partial sequences of *PNPLA2* exon 3 and of the 5′-sequence of the retrotransposon. (D) Agarose gel of PCR fragments showing amplified fragments across the insertion point (from the 5′ end of exon 3 to the transposon) and exon 3 only. The diagram below shows the map of the locus and the locations of the PCR primers. (E) Pedigree of the family based on molecular data.

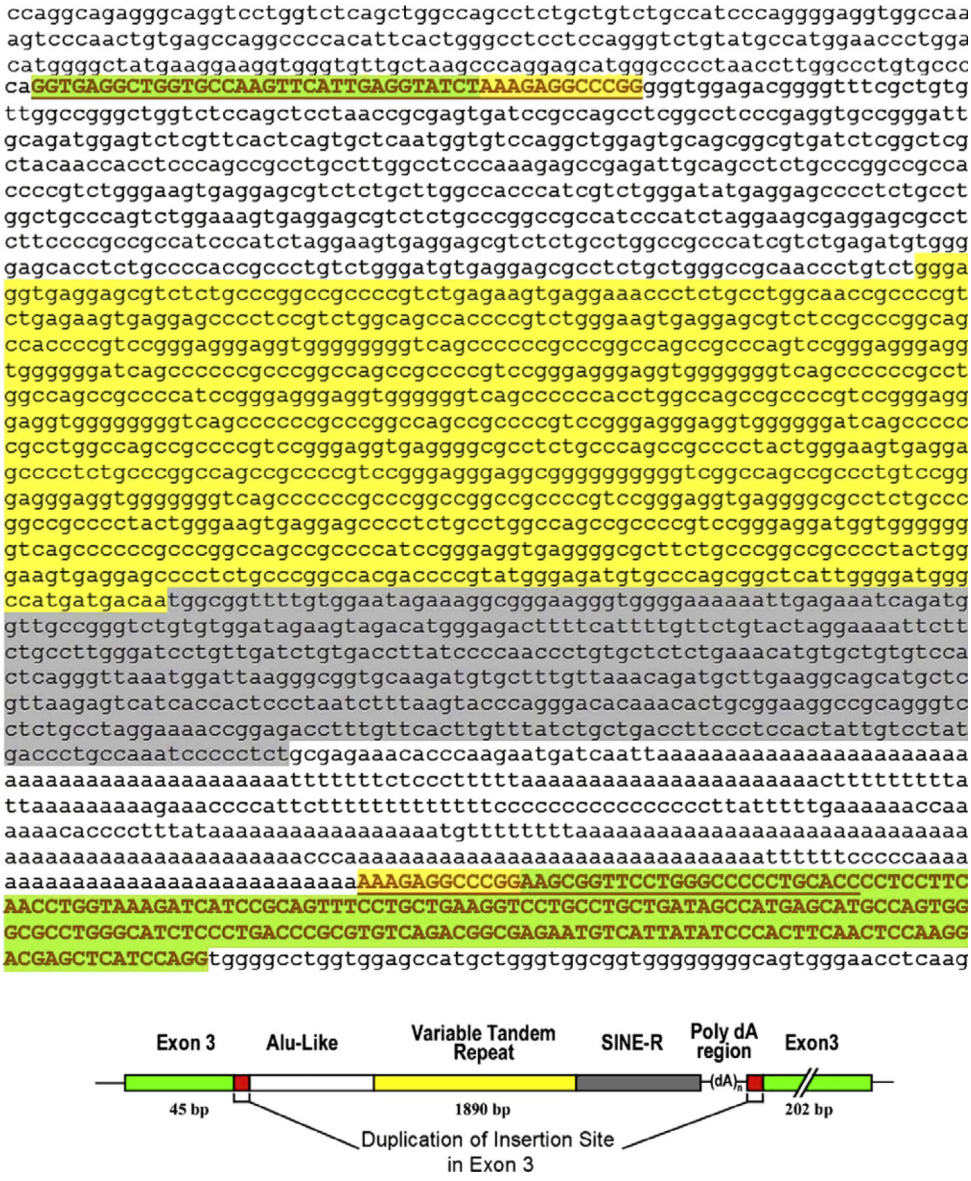

Fig. 5.

Sequence and schematic diagram of the retrotransposon in exon 3 of the *PNPLA2* gene. This element was obtained by PCR amplification of the genomic DNA insert. Sequencing revealed the interruption of exon 3 by a 1890-bp retrotransposon element. This fragment contains a 517-bp *Alu*-like sequence (white bar), an 868-bp sequence of 78% GC-rich variable tandem repeats (yellow bar), and a 431-bp sequence of short interspersed nucleotide elements (gray bar) following a 44-bp poly dA region, all bracketed by the duplicated insertion site (red bar).